Study on the relationship of parameters to steam turbine in the experimental vehicle

S.G. Herawan[1,3,*], K. Talib[2,3], M.M. Tahir[2,3], S.A. Shamsudin[2,3], A. Putra[2,3]

[1)] Faculty of Engineering Technology, Universiti Teknikal Malaysia Melaka, Hang Tuah Jaya, 76100 Durian Tunggal, Melaka, Malaysia.
[2)] Faculty of Mechanical Engineering, Universiti Teknikal Malaysia Melaka, Hang Tuah Jaya, 76100 Durian Tunggal, Melaka, Malaysia
[3)] Centre for Advanced Research on Energy, Universiti Teknikal Malaysia Melaka, Hang Tuah Jaya, 76100 Durian Tunggal, Melaka, Malaysia

[*]Corresponding e-mail: safarudin@utem.edu.my

Keywords: Waste heat recovery; exhaust heat; steam turbine mechanism

ABSTRACT – For a vehicle using internal combustion engine (ICE), the waste energy produced by exhaust can be harness by implementing heat pipe heat exchanger in the automotive system. Water is used as the energy absorption fluid, thus converting the system to steam turbine mechanism that coupling with generator. The paper will explore the parameters that effects the performance of a naturally aspirated spark ignition (S.I.) engine equipped with waste heat recovery mechanism (WHRM). A set of experiments are conduct in order to determine the relationship between parameters (such as engine speed, throttle angle, vehicle speed and exhaust temperature) and steam turbine speed. It is found that the exhaust temperature is expected to give the most significant effect to the steam turbine performance compared to other parameters.

1. INTRODUCTION

The energy from the automotive exhaust can be harness by implementing heat pipe heat exchanger in the automotive system. In order to maximize the amount of waste energy that can be turned to useful energy, the used of appropriate fluid in the heat exchanger is important. Water is used as the fluid, thus converting the system to steam turbine mechanism.

The waste heat energy covers about 70% of fuel energy. Therefore, it is of interest to recover this energy and utilize it to top up the efficiency of overall performance. This is as a waste utilization in term of waste-to-energy like other recycling methods such as carbon molecular sieve from waste of oil palm shell [1] and activated carbon from waste of pinang frond [2].

It has been identified in [3] that the temperature of the exhaust gas varies depending on the engine load and engine speed. As the engine speed increases, the temperature of the exhaust gas will also increase. The recent technologies on waste heat recovery of internal combustion engine (ICE) is consist of low grade heat from cooling system and high grade heat from exhaust system. For low grade waste heat, the organic Rankine Cycle is the favorite choice to recover waste energy [4], whereas high grade heat [5]. In this study, water pump is used in order to produce constant flow of water through the helical copper coil. Note that, the study is done from real condition and on the real road track.

2. METHODOLOGY

The experiment was performed on a Toyota vehicle having 1.6 liter in-line four-cylinder gasoline engines. The detail of running this experimental vehicle can be found in [6]. A schematic diagram of the experimental setup is shown in Figure 1.

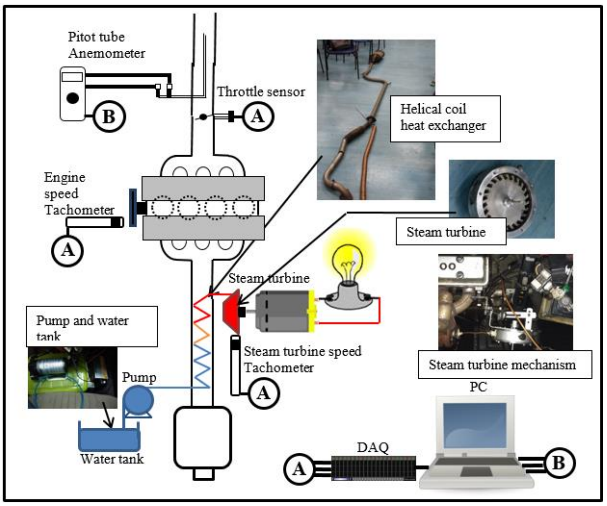

Figure 1 Schematic layout of the experimental setup of waste heat recovery mechanism.

To determine the relationship of parameters to steam turbine speed in the experimental vehicle, a set of test is set up. The water feeding flow rate for this test is constant, that is 60 ml/min. The test will be conducted in 2 rounds. First round, the car will run on the track with normal speed average 60 – 70 km/h and in second round, the car will undergo full-throttle acceleration for about 8 seconds. The detail of the road test can be found in [7].

3. RESULTS AND DISCUSSION

From Figure 2 to 5, the steam turbine speed gradually increased with increasing in other parameters. Then the steam turbine speed gradually increased with increasing in other parameters. Then the steam turbine speed became steady in the range of 18000 to 30000 rpm at 350 to 680 s. This condition occurred during the normal driving test using the experimental vehicle. In the full throttle test, the maximum steam turbine speed could reach up to 33000 rpm.

Meanwhile, Figure 4 shows that from 0 to 210 s, the vehicle speed was 0 km/h. It means the experimental vehicle was not moving or in a full stop position, which did not contribute to higher steam turbine speed compared to normal driving test, even though this test applied higher engine speed up to 5000 rpm, which produced higher exhaust temperature in the range of 280°C to 410°C. This behavior reveals that vehicle speed had a significant effect on the steam turbine speed, whereas the full stop position had minimal influence on the steam turbine speed.

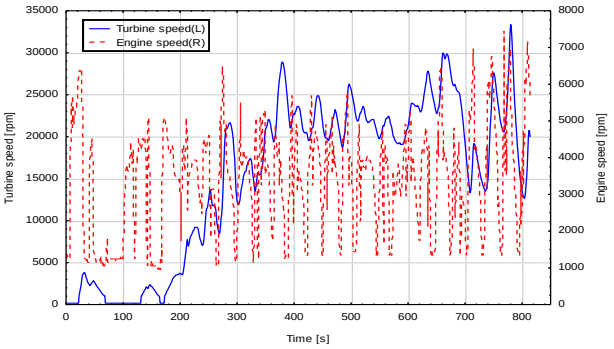

Figure 2 Measured data from experimental vehicle in term of engine speed and steam turbine speed.

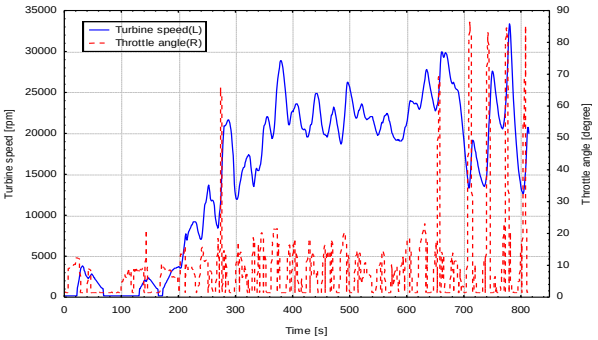

Figure 3 Measured data from experimental vehicle in term of throttle angle and steam turbine speed.

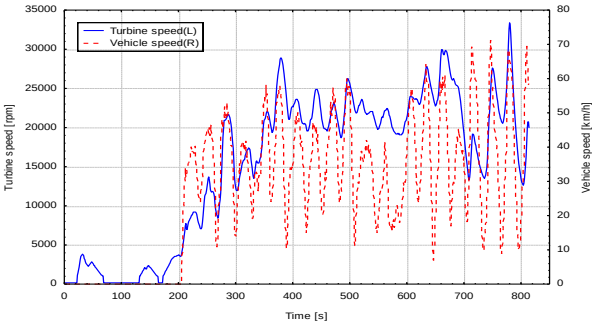

Figure 4 Measured data from experimental vehicle in term of vehicle speed and steam turbine speed.

Compared to other parameters against the steam turbine speed, exhaust temperature had significant effect on the steam turbine speed, where the curve profile of both parameters showed similar behavior (Figure 5). This is due to the enthalpy of steam, which was generated by the exhaust temperature. The higher exhaust temperature can generate higher enthalpy of steam, hence steam turbine speed will increase.

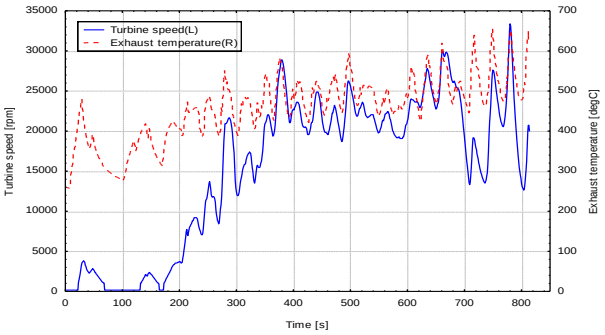

Figure 5 Measured data from experimental vehicle in term of exhaust temperature and steam turbine speed.

4. CONCLUSION

The study of the relationship of parameters to steam turbine in the experimental vehicle has been reported. All four parameters (engine speed, throttle angle, vehicle speed, and exhaust temperature) are proven to give effects on the performance of the steam turbine speed, just the level of significant is different for every parameter. Exhaust temperature is proven to give the most significant effect to the steam turbine performance compared to other parameters.

ACKNOWLEDGMENT

This project is supported by Ministry of Education Malaysia on the Fundamental Research Grant Scheme no. FRGS/2/2014/TK06/FKM/02/F00236.

REFERENCES

[1] Herawan S. G. (2000). Characterisation and analysis of carbon molecular sieve from oil palm shell. Master Thesis.

[2] Herawan S. G., Ahmad M. A., Putra A., & Yusof, A. A. (2013). Effect of flow rate on the pinang frond-based activated carbon for methylene blue removal. The Scientific World Journal, 2013, 1-6.

[3] Peng, Z., Wang, T., He, Y., Yang, X., & Lu, L. (2013). Analysis of environmental and economic benefits of integrated Exhaust Energy Recovery (EER) for vehicles. *Applied Energy*, 105, 238-243.

[4] Boretti, A. A. (2012). Transient operation of internal combustion engines with Rankine waste heat recovery systems. *Applied Thermal Engineering*, 48, 18-23.

[5] Wang, T., Zhang, Y., Zhang, J., Shu, G., & Peng, Z. (2013). Analysis of recoverable exhaust energy from a light-duty gasoline engine. *Applied Thermal Engineering*, 53(2), 414-419.

[6] Herawan, S. G., Rohhaizan, A. H., Putra, A., & Ismail, A. F. (2014). Prediction of waste heat energy recovery performance in a naturally aspirated engine using artificial neural network. *ISRN Mechanical Engineering*, 2014, 1-6.

[7] Herawan, S. G., Rohhaizan, A. H., Ismail, A. F., Shamsudin, S.A., Putra, A., Musthafah, M. T., & Awang, A. R. (2016). Prediction on power produced from power turbine as a waste heat recovery mechanism on naturally aspirated spark ignition engine using artificial neural network. *Modelling and Simulation in Engineering*, 2016, 1-12.

Performance analysis for Peltier module and Seebeck module using Matlab/Simulink

K.N. Khamil[1,2*], M.F.M. Sabri[2], A.M. Yusop[2]

[1)] Department of Mechanical Engineering, University of Malaya, 50603 Kuala Lumpur, Malaysia.
[2)] Faculty of Electronic Engineering and Computer Engineering, Universiti Teknikal Malaysia Melaka, Hang Tuah Jaya, 76100 Durian Tunggal, Melaka, Malaysia

[*]Corresponding e-mail: nisa@utem.edu.my

Keywords: Peltier; Seebeck; analytical modeling; thermoelectric

ABSTRACT – This paper investigates the analytical modelling for both Peltier and Seebeck module available in the market in terms of the coefficient of performance and the efficiency especially in low temperature application using the specification provided by the manufacturer's datasheet. The analytical model helps speed up the investigation on readily available module that suits the researchers need using only Matlab/Simulink. The maximum heat absorbed, Qc obtained is 20.96 W for the Peltier module and the current in Seebeck module are 1.194 A at 6.7 V which confirmed the modelling according to the datasheet provided.

1. INTRODUCTION

Waste heat recovery using thermoelectric (TE) has become an intriguing topic globally with the rising of energy cost and rapid changes in climate. In last decade, researchers have focuses on low ZT materials with large figure of merit in order to achieve high efficiency [1]. Some researchers show the importance of performance improvement through the TE generator system layout itself where some of the layout constructed in three different configurations with different number of module, different temperatures and different airflow rate [1]. There are considerable amount of Peltier and Seebeck module in the market for cooling application and power generation. Even though Peltier modules can be used for power generation by heating up the cold side of the modules, its performance are efficient in the temperature range of 20 °C and 40 °C [2]. Regardless, how much development of TE faces in improving the materials or the TE systems, this helps matured the progress of thermoelectric generators for various applications. In this paper, an analytical modelling for Peltier and Seebeck module are developed using Matlab/Simulink. Thus, it can be a referred easily, to analyze the specific parameters needed for user application using any on-the-shelf module.

2. METHODOLOGY

In this study, analytical modelling is done between Peltier module and Seebeck module where simple methods are shown to estimate the important characteristic between these modules directly from manufacturer datasheets.

2.1 Expression of base dependences for Peltier module

According to previous researches [3-4], features between Peltier and Seebeck module are similar to each other. Most manufacturers of Peltier have set the following parameters to $\Delta T_{\max}$, $V_{\max}$, $I_{\max}$ and the hot side temperature. Therefore, using the data from datasheet, the parameters needed for analytical modeling are:

$$Z = \frac{R_{th}.\alpha_m{}^2}{R_{\text{int}}.} \tag{1}$$

$$\alpha_m = \frac{V_{\max}}{T_h.} \tag{2}$$

$$R_{\text{int}} = \frac{V_{\max}(T_h - \Delta T_{\max})}{I_{\max} T_h.} \tag{3}$$

$$R_{th} = \frac{\Delta T_{\max}}{I_{\max} V_{\max}} \frac{2T_h}{(T_h - \Delta T_{\max})} \tag{4}$$

Where R_{th} is thermal resistivity, R_{int} is total internal resistance of the module and α_m is the Seebeck Coefficient of the module.

The module coefficient of performance can be analyzed using:

$$C.O.P = \frac{Q}{VI.} \tag{5}$$

Where, the expression of voltage, V is

$$V = \frac{2I.R_{\text{int}} + \alpha_m R_{th}(I.R_{\text{int}} + 2\alpha_m T_h)}{2(1 + I.R_{th}.\alpha_m)} \tag{6}$$

2.2 Expression of Base Dependences for Peltier Module

In analyzing Seebeck module, most common specification shown in the manufacturer datasheet would be the match load power, W_m, match load voltage, V_m with given temperature at both hot and cold side, T_h and T_c where some manufacturer provided the optimal efficiency and internal resistance, η_m and R_{int}.

From given specifications, related parameters can be find:

$$Z = \frac{2}{T_h + T_c}\left(\left(\frac{(T_h - T_c) + \eta_m T_c}{(T_h - T_c) - \eta_m T_c}\right)^2 - 1\right) \tag{7}$$

$$\alpha_m = \frac{2V_m}{(T_h - T_c)} \quad (8)$$

$$R_{\text{int}} = \frac{V_m{}^2}{W_m.} \quad (9)$$

But, as the load, R_{load} of the system changes the efficiency changes as well and this effect the R_{th} since $R_{load} = R_{\text{int}}.m$ (1).

$$I = \frac{T_h - T_c}{R_{\text{int}}(1+m)}\alpha_m \quad (10)$$

Therefore, the efficiency $\eta_m = f(I)$ is:

$$\eta(m) = \frac{I^2 R_{\text{int}}}{q_h} = \frac{2.Z.m.(T_h - T_c)}{2(1+m)^2 + Z(T_h + 2mT_h + T_c)} \quad (11)$$

$$R_{th} = \frac{R_{\text{int}}}{\alpha_m{}^2} Z \quad (12)$$

The governing equations for both Peltier and Seebeck modelling are then analyzed using Matlab/Simulink. Numerical simulations are performed to analyze the power generated for low temperature application. The coefficient of performance for the Peltier module and the efficiency for the Seebeck module are evaluated as a function of current.

3. RESULTS AND DISCUSSION

To prove the governing all the equations shown, two on-the-shelf modules are analyzed for power generated between Peltier and Seebeck Module according to Table 1 specifications below.

Table 1 Specifications of Peltier and Seebeck module.

Peltier module	TES1-05350	Seebeck module	TEP1-1994-3.5
$\Delta T_{\max}$	70 °C	V_m	6.7 V
$V_{\max}$	6.8 V	W_m	7.5 W
$I_{\max}$	5 A	T_h	300 °C
T_h	27 °C	Tc	30 °C
		η	5.5%

Figure 1 shows the numerical simulation of the Peltier module as heat absorbed between 27 °C to 45 °C according to the specifications in Table 1. The result of maximum heat absorbed, Qc obtained is 20.96 W which proven the datasheets specification.

While the Figure 2 shows the power curve of the Seebeck module where the current obtained are 1.194 A which confirmed the match load current from the manufacturer's datasheet listed in Table 1.

In the Figure 3 shows the Matlab/Simulink modeling used for Peltier and Seebeck Module.

4. CONCLUSION

In conclusion, the analytical approaches presented in this paper are an easy approach to analyze the performance the module parameters. The maximum heat absorbed, Qc obtained is 20.96 W for the Peltier module and the current in Seebeck module are 1.194 A at 6.7 V which confirmed the datasheets specifications with the analytical simulation made using Matlab/Simulink. The modelling in Matlab can be used to predict which module suitable for the user applications.

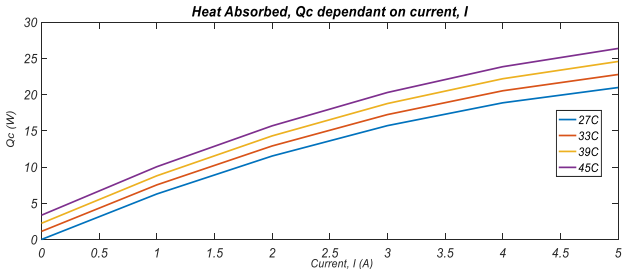

(a)

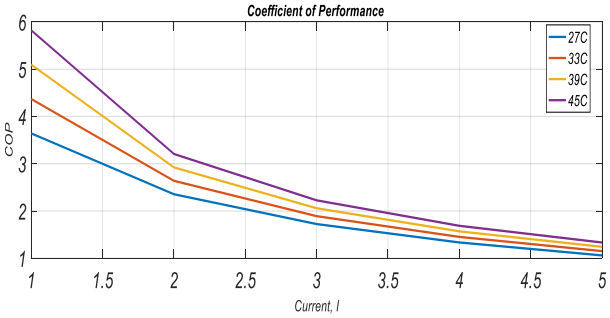

(b)

Figure 1 (a) Coefficient of Performance (COP) and (b) heat absorbed, Qc of the module as a function of the input current, I.

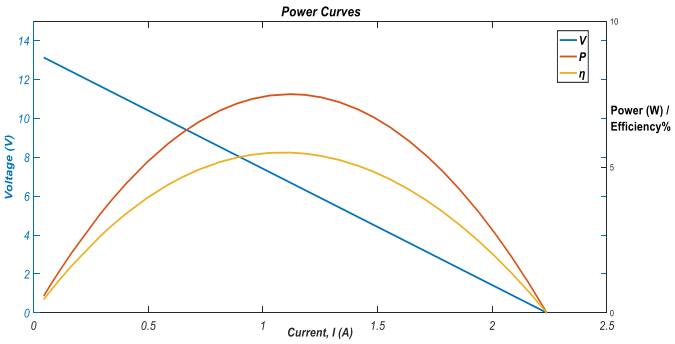

Figure 2 Current-Voltage curve of the Seebeck module.

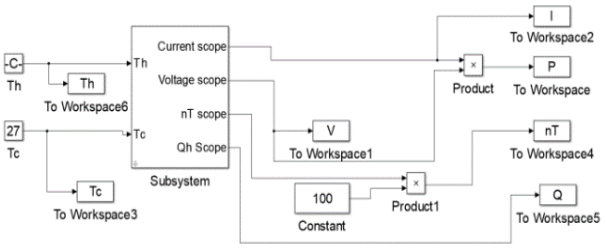

Figure 3 Matlab/Simulink modelling for Peltier and Seebeck module.

ACKNOWLEDGEMENT

This project is supported by Ministry of Education Malaysia (grant number: FRGS/1/2017/TK07/FKEKK-CETRI/F00337) and Universiti Teknikal Malaysia Melaka.

REFERENCES

[1] Twaha, S., Zhu, J., Yan, Y., & Li, B. (2016). A comprehensive review of thermoelectric technology: Materials, applications, modelling and performance improvement. *Renewable and Sustainable Energy Reviews*, *65*, 698–726.

[2] Nesarajah, M., & Frey, G. (2016, October). Thermoelectric power generation: Peltier element versus thermoelectric generator. *Industrial Electronics Society, IECON 2016-42nd Annual Conference of the IEEE*, 4252-4257.

[3] Lineykin, S., & Ben-Yaakov, S. (2007). Modeling and analysis of thermoelectric modules. *IEEE Transactions on Industry Applications*, *43*(2), 505-512.

[4] Belovski, I., Staneva, L., Aleksandrov, A., & Rahnev, P. (2017). Mathematical Model of Thermoelectric Peltier Module. *Journal of Communication and Computer*, *14*, 60-64.

Experimental on Seebeck effect in generating electricity using heat loss at car exhaust system

Mohamad Haniff Harun[1,*], Muhamad Faizal Yaakub[1], Mohd Firdaus Mohd Ab Halim[1], Khalil Azha Mohd Annuar[1], Arman Hadi Azahar[1], Mohd Shahrieel Mohd Aras[2], Amar Faiz Zainal Abidin[1]

[1)] Faculty of Engineering Technology, Universiti Teknikal Malaysia Melaka, Hang Tuah Jaya, 76100 Durian Tunggal, Melaka, Malaysia.
[2)] Faculty of Electrical Engineering, Universiti Teknikal Malaysia Melaka, Hang Tuah Jaya, 76100 Durian Tunggal, Melaka, Malaysia.

[*]Corresponding e-mail: haniff@utem.edu.my

Keywords: Seebeck effect; peltier effect; generating system

ABSTRACT – In the era of globalisation, the electrical energy usage is the main priority in order to do our job and daily activity. Unfortunately, limited power supply for the electrical energy usage makes it hard to continuously provide electrical energy for 24 hours. By using peltier device, it is possible to develop a portable generating system using heat loss in machines and vehicles. The generating system theoretically can recycle the heat loss to produce additional electricity for other usage. Generally, the objective of the generating system is to study on the potential of peltier device to generate useful electricity for additional power supply using heat loss. This generating system can be applied on many types of machines and other type of mechanism such as vehicle that release heat loss. As a result, this system has higher efficiency which 12.59% compared to 6% using proper heat sink using the same module.

1. INTRODUCTION

In Seebeck effect theory, the electrons in the semiconductor act as transferring agent to transfer the heat from one medium to another medium according to the law of thermodynamics. In this case, the application where the energy conversion system applied is on vehicle engines and exhaust system. Based on Electrical Energy Conversion (E2C) past research at the KTH School of Electrical Engineering 2011, all machines are not working 100% effectively, most appears to work only 70% to 80% effectively [1].

Meanwhile, the other 30% to 20% are released into energy loss in term of heat. In order to recover the heat loss, this project will design a portable generating system using peltier device to produce electricity by absorbing heat loss.

There are many applications canned be apply using Peltier device and Seebeck effect. Johari et al. [2] generate voltage by using the TEG Peltier module by heating process using Bunsen burner. The voltage produced by the thermal energy reaction is enough to generate small electricity with value in the range of 1V – 3.75V. Another application and study using Peltier device for producing hot and cold air, as a result system can produce 14°C and up to 56°C [3].

2. METHODOLOGY

Seebeck Effect process involves the electrons in the npn semiconductor to be active and vibrate due to heat then collides with each other in order to release the heat to the cold side. The result is voltage will be produced due to Seebeck effect. The hot side absorbs heat loss at rate of TH high temperature ejected by the system and transfer the heat to the cold side to be released at a rate of TL low temperature. By referring to Seebeck effect, the heat loss absorbed at the hot junction causes electrons to be active and electric current then flow in the npn semiconductor and electrical energy is generated. Using the thermodynamics first law energy conservation principle, the difference between TH and TL will generate the electrical energy output power. The heat released then enter cooling agent which is to maximize the efficiency or the output voltage generated by the device in order to achieve higher temperature gradient between both hot and cold side. The increasing temperature difference between two junctions will increase voltage generation. The generated voltage will flow to the control circuit to provide 12V output voltage to charge battery for other usage [4].

The experimental data are tested at the engine system in order to determine the maximum efficiency for Seebeck Effect. Figure 1 shows the experimental conducted at the engine system.

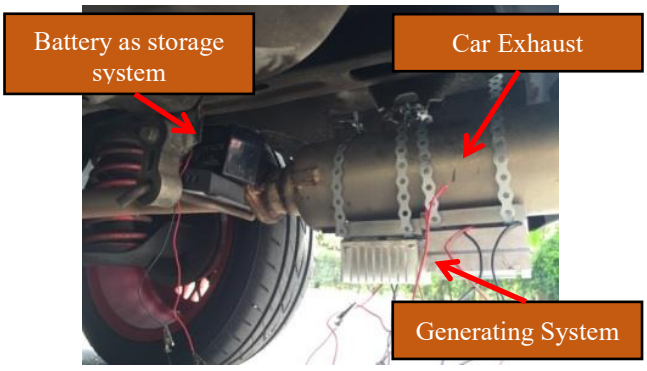

Figure 1 Generating System on Car Exhaust System

The maximum efficiency, η of a peltier device can be defined using the figure of merit, temperatures of the hot side and cold side [3].

$$n_{carnot}\left[\frac{\sqrt{1+Z\bar{T}}-1}{\sqrt{1+Z\bar{T}}+\frac{T_L}{T_H}}\right] \quad (1)$$

Where, T_L is low temperature and T_H is high temperature.

3. RESULTS AND DISCUSSION

The reading was taken at every 5 minutes with total of 30 minutes by considering temperature difference between hot side and cold side is being considered as shown in Table 1. The data was taken when the car stop for every 5 minutes. The car speed was limited to approximately 50 kmh due to the study done in crowded urban areas. Temperature of the surrounding are 32-34 ºC which is unstable. Table 1 shows the data collected at the exhaust system.

The reading was taken at every 5 minutes with total of 30 minutes. The data was taken when the car stop for every 5 minutes. The car speed was limited to approximately 50 kmh. Temperature of the surrounding are 32-34 ºC which is unstable. Table 1 shows the data collected at the engine system.

Table 1 Voltage generated by four peltier modules at exhaust system with temperature difference.

Time (min)	Voltage (V)	$T_{Difference}$ (ºC)
0	0	0
5	2.43	18
10	5.82	37
15	8.99	54
20	12.54	71
25	12.76	93
30	12.76	112

Based on the data collected, the generating system with four number of TEC1-12706 modules able to generate voltage up to 12.76 V maximum starting from 25 minutes. As the car exhaust system become hotter, the temperature difference between hot and cold side of the generating system increases. From the Figure 3, the value of voltage generated, and temperature difference are increasing over time then voltage generated reach its maximum value 12.76V due to the maximum operating for four Peltier device.

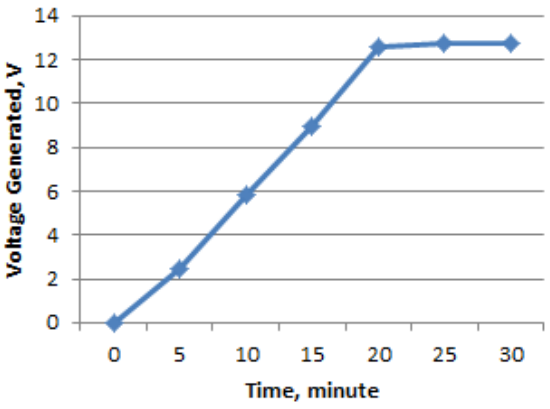

Figure 3 Voltage generated at exhaust system.

From the efficiency of Carnot, the maximum efficiency of the Peltier TEC1-12706 using Equation (1) calculated as shown below.

$$N = (0.7481)\left[\frac{\sqrt{1+0.5711}-1}{\sqrt{1+0.5711}+\frac{33}{131}}\right]=12.59\% \quad (2)$$

By comparing the maximum efficiency of this generating system to past research by researcher [5], this generating system has higher efficiency which 12.59% compared to 6% using proper heat sink with the same module TEC1-12706.

4. CONCLUSION

In conclusion, peltier modules TEC1-12706 are able to generate voltage from the heat loss at car exhaust system. Therefore, the potential of peltier in generating electricity is accepted and the generating systems are effectively generates electricity from the heat loss of the vehicle system.

ACKNOWLEDGEMENT

We wish to express our gratitude to MOHE, Universiti Teknikal Malaysia Melaka (UTeM) especially for Centre for Robotics and Industrial Automation (CeRIA), Centre of Research and Innovation Management (CRIM) and to Faculty of Engineering Technology from UTeM to give the financial (RAGS/1/2015/TK0/FTK/03/B00114) as well as moral support for complete this project successfully.

REFERENCES

[1] Ramade, P., Patil, P., Shelar, M., Chaudhary, S., Yadav, S., & Trimbake, S. (2014). Automobile exhaust thermo-electric generator design & performance analysis. *International Journal of Emerging Technology and Advanced Engineering*, *4*(5), 682-691.

[2] Johari, S. H., Pa, M. F. C., Annuar, K. A. M., Ahmad, S., & Zahari, M. (2016). Performance analysis of portable power generator by using TEG module. *Proceedings of Mechanical Engineering Research Day*, *2016*, 79-80.

[3] Harun, M. H., Annuar, K. A. M., Halim, M. F. M. A., Hasan, M. H. C., Aras, M. S. M., & Yaakub, M. F. (2016). Peltier and seebeck efficacy of hot and cold air system for portable O-REF (oven & refrigerator) application. *Proceedings of Mechanical Engineering Research Day*, *2016*, 81-82.

[4] Ozollapins, M., & Kakitis, A. (2012). Thermoelectric generators as alternate energy source in heating systems. *Engineering for Rural Development, 24,* 673-677.

[5] Peter, A. J. D., Balaji, D., & Gowrishankar, D. (2013). Waste heat energy harvesting using thermo electric generator. *IOSR Journal of Engineering (IOSRJEN), 3*, 1-4.

Thermogravimetric analysis of mangrove wood

H. Ghafar[1,*], R. Zailani[2]

[1)] Faculty of Mechanical Engineering, Universiti Teknologi MARA, Cawangan Pulau Pinang, Jalan Permatang Pauh, 13500 Permatang Pauh, Pulau Pinang, Malaysia.
[2)] Faculty of Mechanical Engineering, Universiti Tekologi MARA, 40450 Shah Alam, Selangor, Malaysia.

[*]Corresponding e-mail: halim4346@ppinang.uitm.edu.my

Keywords: Thermogravimetric analysis; mangrove wood; biomass

ABSTRACT – Mangrove wood is recognized as potential biomass resource that was used for charcoal and pole production in Malaysia. Thermal characteristics of mangrove wood was studied by conducting thermogravimetric analysis (TGA). It was found that volatile matter, fixed carbon and ash, moisture content contributes 55.65%, 21.61%, 7.24% to the contents of mangrove wood. The results proved that the mangrove wood can be used as one of the resources for biomass energy.

1. INTRODUCTION

Forest residues is one of renewable energy sources with the biggest renewable energy value in Malaysia, generates annual income of estimated RM11984 million as shown in Table 1 [1]. One of forest residues that are well known in Malaysia is mangrove wood. Mangrove wood is one of potential biomass resource that was used as charcoal and pole production [2] especially in Malaysia. Southeast Asia has the largest area of mangrove tree, while Malaysia has the 3rd largest area of mangrove tree [3]. This indicates the potential of mangrove wood as biomass resource in Malaysia.

Mangrove wood has significant calorific value between 17.23 MJ/kg to 19.21 MJ/kg [4] compare to any other woods which vary between 17.9 MJ/kg to 20.5 MJ/kg [5]. Thermal characteristic study of mangrove wood is important in determining the suitable thermal conversion process, such as pyrolysis, gasification etc to convert into more useful energy such as solid fuel, liquid fuel. The objective of this paper is to study on the thermal characteristics of mangrove wood using thermogravimetric analysis (TGA).

Table 1 Types of renewable energy in Malaysia and its energy value [1].

Renewable energy sources	Energy value in RM million (annual)
Forest Residues	11984
Oil Palm Biomass	6379
Solar Thermal	3023
Mill Residues	836
Hydro	506
Solar PV	378
Municipal Waste	190
Rice Husk	77
Landfill Gas	4

2. METHODOLOGY

Sample of mangrove wood was obtained from mangrove forest near Port Klang. The samples were cut small into 1cm^3 cube size and dried in the oven at 50 °C for 24 hours. The dried samples were grounded into powder using crusher. Proximate analysis was done using Thermogravimetric analysis (TGA) method.

In TGA method, the content and thermal characteristics of mangrove wood was analysed and performed on TGA analyser model Pyris1 as shown in Figure 1. 20 mg of samples were placed in the cup holder inside the analyser. It was then heated under heating rate at about 10K/min from room temperature until it reached 800 °C. It was conducted according to ASTM D 5865-11a [6].

Figure 1 TGA analyser.

3. RESULTS AND DISCUSSION

Figure 2 show the thermogravimetric analysis result for mangrove wood. Thermogravimetric (TG) profile gives thermal characteristics of mangrove wood. Different biomass would give different TG profile as the contents of hemicellulose, cellulose and lignin are different type of biomass.

Initial weight loss of mangrove wood was 7.41% that was observed at 130 °C as shown in Figure 2. This was due to the moisture loss of mangrove wood. It was later noticed that there was maximum weight loss at about 53.86% occurred at temperature range between 180°C and 460 °C. This was due to the devolatilization of mangrove wood. It leaves 17.11% of the remaining residue that consisted of fixed carbon and ash content.

Mangrove wood devolatilization can be seen on DTG curve in Figure 2 that revealed 2 peaks pattern. The

first stage of devolatilization occurred at temperature range between 180℃ and 280℃. This was followed by the second stage of devolatilization at temperature range between 280℃ and 460℃. The first stage of devolatilization was due to decomposition of hemicellulose while the second stage of devolatilization was due to decomposition of cellulose. The highest peak of the first stage was hardly noticed at 270℃ at rate 3.4%/min. The highest peak of second stage was almost 2 times higher than the first occurred at 340℃ at rate 6.5%/min. The devolatilization process of mangrove wood completed at 600 ℃.

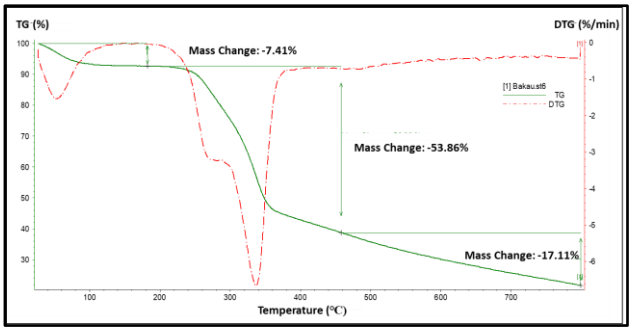

Figure 2 Thermogravimetric analysis of mangrove wood.

Based on Table 2, it is observed from proximate analysis that mangrove wood contains volatile matter, fixed carbon and ash, and moisture content. Volatile matter contributed significantly in the content for about 55.65%. Fixed carbon and ash content of mangrove wood was 21.61% while moisture content at 7.24%. Previous study shown the similar amount of moisture content but different amount of volatile matter, fixed carbon and ash content[7]. This was due to different type of mangrove wood could contribute to this major difference of values. In general, the same pattern can be observed as volatile matter contribute highest content, followed by fixed carbon and ash, and moisture content.

Table 2 Comparison between values obtain from experiment and from previous studies.

Proximate analysis	**Mangrove wood (%)**	**Reference value (%)***
Volatile matter	55.65	73.50
Fixed carbon and ash	21.61	19.00
Moisture	7.24	7.50

*Source [7]

4. CONCLUSION

In conclusion, TGA analysis obtained shows that there were two groups of reactions in devolatilization process of mangrove wood which can translated by the appearance of two peaks of devolatilization rate. Volatile matter contributed 55.65% to the total content of mangrove wood. Fixed carbon and ash contributed 21.61% while moisture contributed 7.25%. Higher content of volatile matter shows that mangrove wood is suitable for the production of biofuel, while fixed carbon content contribute to the higher production of solid fuels.

ACKNOWLEDGEMENT

The financial support from MOHE through The Research Management Institute, Universiti Teknologi MARA Malaysia, FRGS (600-RMI/ST/FRGS 5/3Fst(89/2010), is highly appreciated.

REFERENCES

[1] Sumathi, S., Chai, S. P., & Mohamed, A. R. (2008). Utilization of oil palm as a source of renewable energy in Malaysia. *Renewable and Sustainable Energy Reviews*, *12*(9), 2404-2421.

[2] Chong, V. C. (2006). Sustainable utilization and management of mangrove ecosystems of Malaysia. *Aquatic Ecosystem Health & Management*, *9*(2), 249-260.

[3] Hutchison, J., Manica, A., Swetnam, R., Balmford, A., & Spalding, M. (2014). Predicting global patterns in mangrove forest biomass. *Conservation Letters*, *7*(3), 233-240.

[4] Lin, Y., Lin, P., & Wang, T. (2000). Caloric values and ash contents of some mangrove woods. *The Journal of Applied Ecology*, *11*(2), 181-184.

[5] Günther, B., Gebauer, K., Barkowski, R., Rosenthal, M., & Bues, C. T. (2012). Calorific value of selected wood species and wood products. *European Journal of Wood and Wood Products*, *70*(5), 755-757.

[6] Standard, A. S. T. M. (2007). A standard test method for gross calorific value of coal and coke. *ASTM D5865*.

[7] Said, M. M., Mhilu, C. F., John, G. R., & Manyele, S. (2014). Analysis of pyrolysis kinetics and energy content of agricultural and forest waste. *Open Journal of Renewable Energy and Sustainable Development, 1*(1), 36-44.

Energy audit in public higher learning institution: A case for chancellery building

M.I.M. Hafiz[1,2,*], M.F. Sulaima[1], J.A. Razak[1], M.M. Tahir[1,2], Z.H. Bohari[1], M.K.M. Nor[1], A. Othman[1], S.R. Omar[1]

[1)] Center for Sustainability and Environment, Universiti Teknikal Malaysia Melaka, Hang Tuah Jaya, 76100 Durian Tunggal, Melaka, Malaysia.
[2)] Centre for Advanced Research on Energy, Universiti Teknikal Malaysia Melaka, Hang Tuah Jaya, 76100 Durian Tunggal, Melaka, Malaysia.

[*]Corresponding e-mail: mohamedhafiz@utem.edu.my

Keywords: Energy audit; public higher learning institution; Chancellery building

ABSTRACT – Malaysia has voluntarily pledge to reduce its carbon emission intensity in 2030 by 45% compare to a baseline set in 2005. Energy consumption from higher learning institution building is one of the contributor to the carbon emission. Therefore, implementation of energy audit is essential to define the energy losses and develop energy conservation and saving initiatives. The result indicates that annual energy consumption is 1,887,700 kWh, with Building Energy Index (BEI) of 261.73 kWh/m^2/y. Nine (9) energy conservation measures has been identified to reduce the energy consumption. The payback period for the measures implementation is within less than 2.2 years with potential saving is 33%.

1. INTRODUCTION

Malaysia has pledge to reduce its carbon emission intensity of Gross Domestic Products (GDP) by 45% by 2030 relative to the emission intensity of GDP in 2005 [1]. In achieving this target, 11th Malaysia Plan has set 10 strategic thrusts which include the pursuing green growth for sustainability and resilience which has become the 6th strategic trust. Under this thrust, adopting the sustainable production and consumption has been put as one of the key focus area which embedded the enhancing demand side management of energy consumption [2].

One of the key initiative is the implementation of Energy Audit Conditional Grant Program which a 3 years program from 2016 until 2018 aim to create awareness, provide financing assistance, attract financial institution and develop capacity building for audited building and energy service company. Therefore, Universiti Teknikal Malaysia Melaka (UTeM) took this initiative to conduct energy audit at Chancellery Building. The building was established on 8 July 2009 and it started operation on 29 September 2009 and function as a administrative building for a university with Net Floor Area (NFA) of 7,212.25m^2. The building main energy supply are in the form of electricity from TNB (100%).

2. METHODOLOGY

The important steps involve in conducting the energy audit as follows:

1. Desktop data collection;
2. Review of building operation and utilization factor;
3. On site measurement; and
4. Development of energy conservation measures.

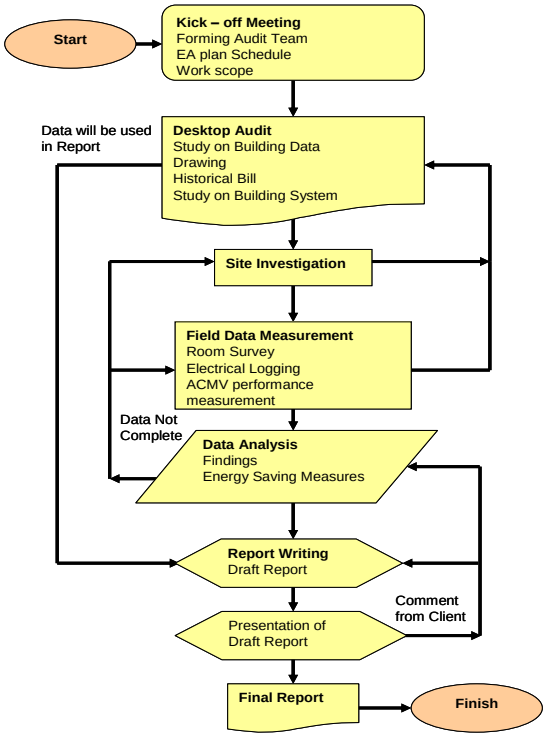

Figure 1 Energy audit flow chartFigure 1 shows the energy audit flow chart at the Chancellery UTeM. The onsite measurement has been conducted for two weeks from 11th until 25th November 2016. The process was strictly follow from the guidebook published by Energy Commission (EC) [3].

3. RESULTS AND DISCUSSION

3.1 Historical bill analysis

The annual energy consumption at Chancellery UTeM is 1,887,700 kWh which is equivalent to RM 689,010.50. Figure 2 shows the monthly energy consumption at Chancellery UTeM. Based on the figure, the average energy consumption is 157,308 kWh while the highest energy consumption is in October 2014. On the other hand, the lowest energy consumption is in June 2015. This is related with the number of cooling degree days (CDD), number of working days, number of days in month and number of class day at UTeM.

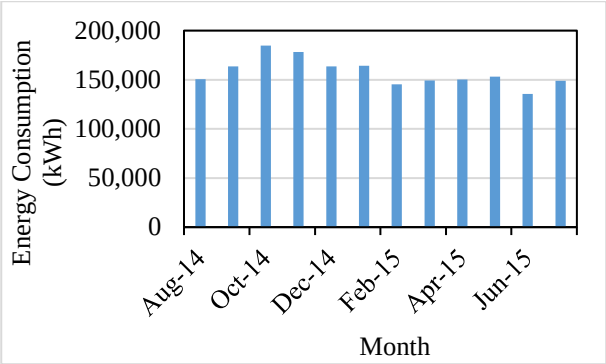

Figure 2 Monthly energy consumption at Chancellery UTeM.

Further analysis was performed to determine the correlation between the energy consumption and the impact independent variables, namely CDD, number of days in month, working days and number of class days. Multiple linear regression was performed by combining both independent variables. The result indicates that the multiple regression value (R) is 0.68 and the baseline energy consumption equation as Equation (1):

$$y = 3090x_1 + 5060x_2 + 457x_3 - 392x_4 + 10604 \quad (1)$$

Where;

$y = \text{energy consumption, kWh}$
$x_1 = \text{number of working day}$
$x_2 = \text{number of days in month}$
$x_3 = \text{number of class day}$
$x_4 = \text{cooling degree days}$

3.2 Power load apportioning

Load apportioning analysis was performed to identify the highest power demand in the building. Figure 3 shows that highest power demand is from air conditioning unit comprising the air handling unit, chilled water pump and suction water pump. Next, the power demand used for lighting followed by others such as plug load. Therefore, the energy conservation measures should have focus on air conditioning unit to gain significant reduction of energy consumption.

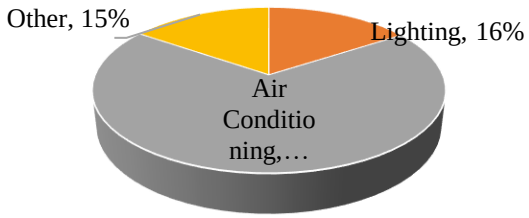

Figure 3 Power load apportioning at Chancellery UTeM.

3.3 Energy conservation measures (ECMs)

The development of ECMs is based on the technical and financial constraint found at Chancellery UTeM. The financial is evaluated by the duration of payback period as per. Table 1.

Table 1 ECMs suggestion for Chancellery UTeM.

Energy conservation measures	Potential saving		Investment (RM)	Pay-back period (year)
	Energy (kWh)/ year	Cost (RM)/ year		
Improving SEMS	94,385	34,451	15,000	0.44
Control & Monitoring of base load	140,361	51,232	9,000	0.18
Lighting Retrofit FL(36W) to LED(20W)	123,402	45,042	173,040	3.84
Lighting Retrofit FL(18W) to LED(10W)	4,118	1,503	10,725	7.13
Remove Unnecessary Lighting by De-lamping	58,359	21,301	N/A	N/A
VFD for AHU Motor	100,289	53,302	280,000	5.25
Comprehensive Cleaning for Chiller	20,437	7,459	18,000	2.41
Comprehensive Cleaning for Cooling Tower	35,197	12,847	10,000	0.78
Sensor Upgrade for HVAC System	49,974	18,245	8,000	0.44
Total	**622,352**	**243,855**	**523,765**	**2.15**

Overall, 9 ECMs were suggest for Chancellery UTeM. Total investment requires to implement all the 9 ECMs is RM 523,765 with payback period is less than 2.2 years. Total energy and cost saving is 622,352 kWh/year and RM 243,855 respectively. The targeted Building Energy Index (BEI) reduce from 262 kWh/m^2/year to 175 kWh/m^2/year.

4. CONCLUSION

In conclusion, total potential energy saving for Chancellery UTeM if all the ECMs implement is approximately 33% while for the cost reduction is 35.39% congruently.

REFERENCES

[1] New Straits Times Onlines, "Malaysia is on track to hit carbon emission reduction target: PM Najib," Media Prima Berhad, 19/03/2016. [Online]. Available: http://www.nst.com.my/news/2016/03/133719/malaysia-track-hit-carbon-emission-reduction-target-pm-najib.

[2] Malaysia Economic Planning Unit, "11th Malaysia Plan," 21/05/2015. [Online]. Available: http://www.micci.com/downloads/11MP.pdf.

[3] Malaysia Energy Commission , Electrical Energy Audit Guidelines for Building, Putrajaya: Malaysia Energy Commission , 2016.

Energy audit in public higher learning institution: A case for library

M.I.M. Hafiz[1,2,*], M.F. Sulaima[1], J.A. Razak[1], M.M. Tahir[1,2], Z.H. Bohari[1], M.K.M. Nor[1], A. Othman[1], S.R. Omar[1]

[1)] Center for Sustainability and Environment, Universiti Teknikal Malaysia Melaka, Hang Tuah Jaya, 76100 Durian Tunggal, Melaka, Malaysia.
[2)] Centre for Advanced Research on Energy, Universiti Teknikal Malaysia Melaka, Hang Tuah Jaya, 76100 Durian Tunggal, Melaka, Malaysia.

[*]Corresponding e-mail: mohamedhafiz@utem.edu.my

Keywords: Energy audit, public higher learning institution, library

ABSTRACT – Malaysia has voluntarily pledge to reduce its carbon emission intensity in 2030 by 45% compare to a baseline set in 2005. Energy consumption from higher learning institution building is one of the contributor to the carbon emission. Therefore, implementation of energy audit is essential to define the energy losses and develop energy conservation and saving initiatives. The result indicates that annual energy consumption is 1,374,110 kWh, with Building Energy Index (BEI) of 172.26 kWh/m^2/y. Eleven (11) energy conservation measures has been identified to reduce the energy consumption. The payback period for the measures implementation is within less than 2.01 years with potential saving is 28%.

1. INTRODUCTION

Malaysia has pledge to reduce its carbon emission intensity of Gross Domestic Products (GDP) by 45% by 2030 relative to the emission intensity of GDP in 2005 [1]. In achieving this target, 11th Malaysia Plan has set 10 strategic thrusts which include the pursuing green growth for sustainability and resilience which has become the 6th strategic trust. Under this thrust, adopting the sustainable production and consumption has been put as one of the key focus area which embedded the enhancing demand side management of energy consumption [2].

One of the key initiative is the implementation of Energy Audit Conditional Grant Program which a 3 years program from 2016 until 2018 aim to create awareness, provide financing assistance, attract financial institution and develop capacity building for audited building and energy service company. Therefore, Universiti Teknikal Malaysia Melaka (UTeM) took this initiative to conduct energy audit at Perpustakaan Laman Hikmah (PLH). The building was established on 8 July 2009 and it started operation on 29 September 2009 and function as a library with Net Floor Area is 7,977 m^2. The building main energy supply are in the form of electricity from TNB (100%).

2. METHODOLOGY

The important steps involve in conducting the energy audit as follows:

1. Desktop data collection;
2. Review of building operation and utilization factor;
3. On site measurement using PEL 103 Power Logger ; and
4. Development of energy conservation measures.

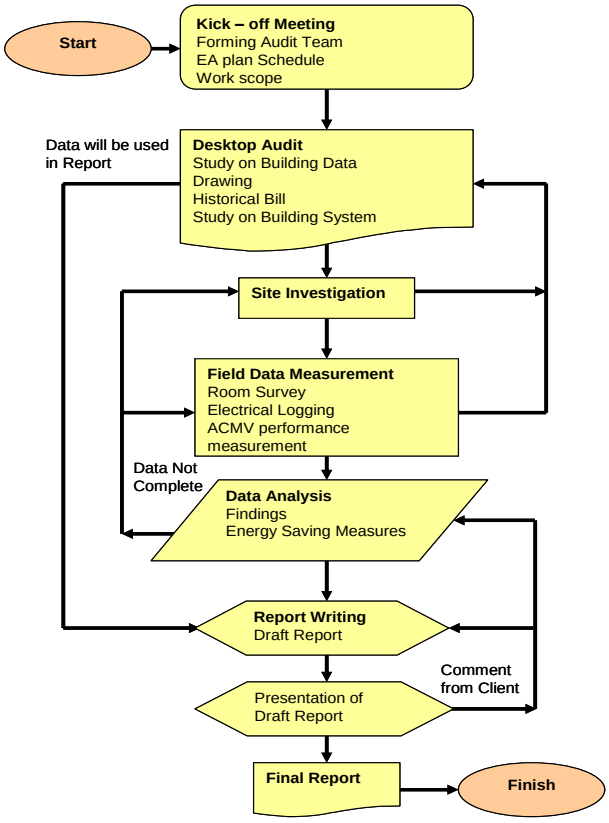

Figure **1** Energy audit flow chart.Figure **1** shows the energy audit flow chart at the PLH, UTeM. The onsite measurement has been conducted for two weeks from 26th October until 9th November 2016. The process was strictly follow from the guidebook published by Energy Commission (EC) [3].

3. RESULTS AND DISCUSSION

3.1 Historical bill analysis

The annual energy consumption at PLH UTeM is 1,374,110 kWh which is equivalent to RM 501,550.15. Figure 2 shows the monthly energy consumption at PLH UTeM. Based on the figure, the average energy consumption is 114,509 kWh while the highest energy consumption is in April 2015. On the other hand, the lowest energy consumption is in February 2015. This is related with the number of cooling degree days (CDD), number of working days, number of days in month and number of class day at UTeM.

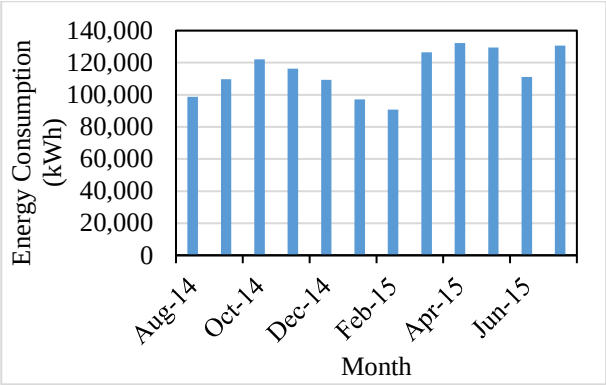

Figure 2 Monthly energy consumption at PLH UTeM.

Further analysis was performed to determine the correlation between the energy consumption and the impact independent variables, namely CDD, number of days in month, working days and number of class days. Multiple linear regression was performed by combining both independent variables. The result indicate that the multiple regression value (R) is 0.86 and the baseline energy consumption equation as Equation (1) where:

$$y = 2879x_1 - 652x_2 + 450x_3 + 405x_4 - 24055 \quad (1)$$

$y = \text{energy consumption, kWh}$
$x_1 = \text{number of working day}$
$x_2 = \text{number of days in month}$
$x_3 = \text{number of class day}$
$x_4 = \text{cooling degree days}$

3.2 Power load apportioning

Load apportioning analysis was performed to identify the highest power demand in the building. Figure 3 shows that highest power demand is from air conditioning unit comprising the air handling unit, chilled water pump and suction water pump. Next, the power demand used for lighting followed by others such as plug load. Therefore, the energy conservation measures should have focus on air conditioning unit to gain significant reduction of energy consumption.

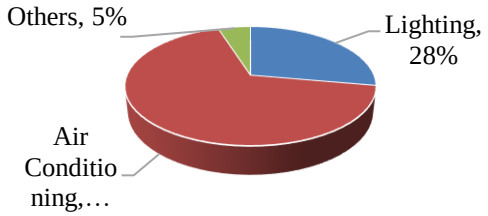

Figure 3 Power load apportioning at PLH UTeM

3.3 Energy conservation measures (ECMs)

The development of ECMs is based on the technical and financial constraint found at PLH UTeM. The financial is evaluated by the duration of payback period as per. Table 1.

Table 1 ECMs suggestion for PLH UTeM.

Energy conservation measures	Potential saving		Investment (RM)	Pay-back period (year)
	Energy (kWh)/ year	Cost (RM)/ year		
Improving SEMS	68,706	25,078	15,000	0.60
Control & Monitoring of base load	59,278	21,637	9,000	0.42
Lighting Retrofit FL(36W) to LED(20W)	66,298	24,199	80,570	3.33
Lighting Retrofit FL(18W) to LED(10W)	2,678	978	6,045	6.18
Remove Unnecessary Lighting by De-lamping	40,195	14,671	N/A	N/A
VFD for AHU Motor	57,845	29,622	117,000	3.95
Comprehensive Cleaning for Chiller	14,888	5,434	18,000	3.31
Comprehensive Cleaning for Cooling Tower	12,074	4,407	10,000	2.27
Avoid To Operate 2 Cooling Tower	11,351	4,143	N/A	N/A
New Cooling system Coolsure (Book Storage)	27,419	10,008	32,000	3.20
Sensor Upgrade for HVAC System	18,610	6,793	8,000	1.18
Total	**379,340**	**146,967**	**295,615**	**2.01**

Overall, 11 ECMs were suggest for Library UTeM. Total investment requires to implement all the 11 ECMs is RM 295,615 with payback period is within 2.01 years. Total energy and cost saving is 379,340 kWh/year and RM 146,967 respectively. The targeted BEI reduce from 172 kWh/m^2/year to 124 kWh/m^2/year.

4. CONCLUSION

In conclusion, total potential energy saving for PLH UTeM if all the ECMs implement is approximately 28% while for the cost reduction is 29.3% congruently.

REFERENCES

[1] New Straits Times Onlines, "Malaysia is on track to hit carbon emission reduction target: PM Najib," Media Prima Berhad, 19/03/2016. [Online]. Available: http://www.nst.com.my/news/2016/03/133719/malaysia-track-hit-carbon-emission-reduction-target-pm-najib.

[2] Malaysia Economic Planning Unit, "11th Malaysia Plan," 21/05/2015. [Online]. Available: http://www.micci.com/downloads/11MP.pdf.

[3] Malaysia Energy Commission , Electrical Energy Audit Guidelines for Building, Putrajaya: Malaysia Energy Commission , 2016.

Effect of alkali on decomposition of cellulose for hydrogen production by using RF plasma in liquid

Fadhli Syahrial[1,2,*], Shinfuku Nomura[3], Fudhail Abdul Munir[1,2], Shinobu Mukasa[3], Hiromichi Toyota[3], Kazuki Tange[3]

[1)] Faculty of Mechanical Engineering, Universiti Teknikal Malaysia Melaka,
Hang Tuah Jaya, 76100 Durian Tunggal, Melaka, Malaysia.
[2)] Centre for Advanced Research on Energy, Universiti Teknikal Malaysia Melaka,
Hang Tuah Jaya, 76100 Durian Tunggal, Melaka, Malaysia.
[3)] Department of Mechanical Engineering, Graduate School of Science and Engineering, Ehime University,
3 Bunkyo-cho, Matsuyama 790-8577, Ehime, Japan.

[*]Corresponding e-mail: fadhlisyahrial@utem.edu.my

Keywords: Hydrogen; plasma in liquid; cellulose

ABSTRACT – Hydrogen shows great promise for being such a solution for providing sustainable energy while at the same time protecting the environment from greenhouse gases (GHGs). A 27.12 MHz RF plasma in liquid was used to decompose biomass-derived cellulose suspension for hydrogen production. At 1.0 M of sodium hydroxide, the result showed the highest hydrogen yield and the lowest greenhouse gases yield. An increase in molar concentration resulted in an increase of hydrogen production rate. On the other hand, it is noted that regardless of molar concentration, the hydrogen production rate significantly dropped with residence time.

1. INTRODUCTION

Plasma in liquid is a process in which plasma is generated inside a bubble produced by evaporation of a surrounding liquid by the heat of plasma. Nomura and Toyota was succeed in depositing diamond like carbon 9000 times faster than gas-phase plasma by applying plasma in liquid in a *n*-dodecane irradiated simultaneously by microwave and ultrasonic waves [1]. The existence of radical species such as H radicals and hydroxyl radicals inside the bubbles seems more favorable for higher reaction rates than those for conventional gas-phase plasma [2]. In our previous study, hydrogen was produced from glucose solution by using 27.12 MHz RF plasma in liquid with 29 kHz ultrasonic irradiation [3].

In this study a 24.12 MHz radio frequency (RF) plasma in liquid was employed to decompose biomass-derived cellulose suspension for hydrogen production. The effect of sodium hydroxide as an alkali solvent on hydrogen production rate and yield was observed.

2. METHODOLOGY

Decomposition of cellulose suspension for hydrogen production was conducted by using radio-frequency (RF) in-liquid plasma, as depicted in Fig. 1. A 3.0 mm diameter copper rod was employed as an electrode. The copper electrode was encased in a glass tube as a dielectric substance to avoid energy loss. A counter electrode was fixed to the top of reactor vessel with the distance 26 mm from the tip of copper electrode.

Plasma was generated at the tip of copper electrode at atmopsheric pressure. An aspirator was employed to reduce the reactor pressure to 0.01-0.02 MPa. The impedance and power input of matching box and 27.12 MHz RF generator, respectively were simultaneously adjusted for the generation of plasma in liquid. The discharged power was 150 W, as calculated by subtraction of the reflected power from the generated power.

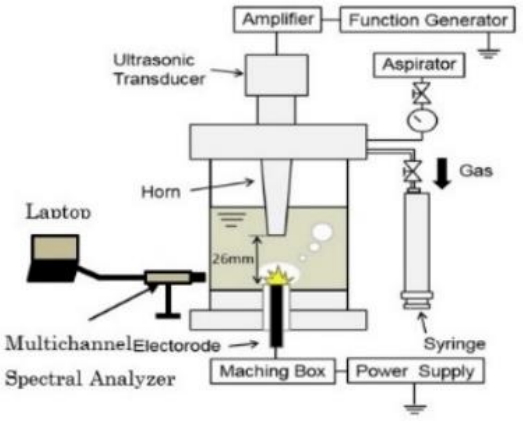

Figure 1 RF plasma in liquid.

In this study, sodium hydroxide was used as an alkali solvent to enhance the chemical reaction in decomposition process of cellulose suspension by plasma. Initially, the experiments were conducted to observe the effect of alkali on decomposition of cellulose suspension. The sample of the suspension were mixed with 0.01, 0.1 and 1.0 M of sodium hydroxide. The volume of the suspensions were prepared for 120 mL and the initial concentrations of cellulose suspension were varied between 0.5 and 20.0 wt%. Next, sulfuric acid (1.0 M) was used as a solvent to observe the effect between alkali and acid on decomposition of cellulose suspension. Cellulose powder provided by Wako Pure Chemical Industries, Japan was employed.

Plasma generation induced radical species. The existence of radical species was measured using a multichannel spectral analyzer (Hamamatsu PMA-11C7473-36) and the values used are the average values for 5 repititions over a sampling time of 0.5 s.

The gas production rate was measured for every 1 minute and was drawn out of the apparatus by a gas-tight glass syringe 20 min after the reaction reached

atmospheric pressure. Then, the gas produced was measured using a gas chromatograph (GC-8A Shimadzu). Argon gas was used as the carrier gas in the chromatograph.

3. RESULTS AND DISCUSSION

3.1 Plasma diagnostics

A typical spectrum emitted by the water decomposition by plasma is shown in Figure 2. As it can be seen, the dominant spectrums were Hα (656.3 nm) and OH (281.1 nm). The spectrum also contained H_β (486 nm). Since both bands did not interfere with each other, they could be employed for temperature determination. The electron temperature was estimated to be 4200 K, obtained from the ratio of the emission intensity of Hα and H_β by using Boltzmann plot equation [2], [4]. Dissociation of water in a plasma discharge also produced other radical species such as oxygen atom (O) and H_2O^+ [5].

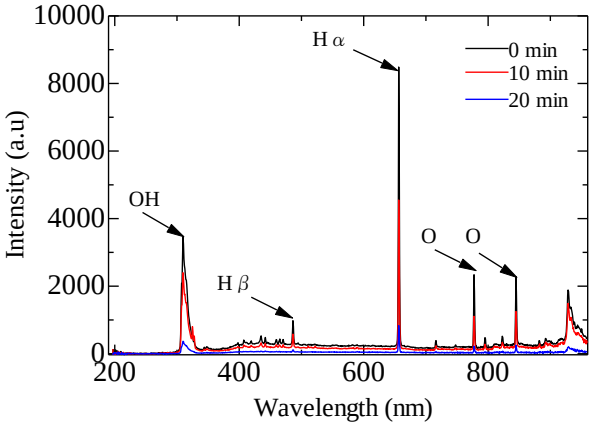

Figure 2 Emission spectrum of H_2O RF plasma in liquid.

The optical emission spectrum shows that the intensity of all reactive species relatively changes with residence time. As the residence time increase, the intensity of all radical species lines decreased, indicating that the plasma source was less efficient for producing radical species. It was occurred due to the erosion at the tip of the electrode which made of Cu.

3.2 Effect of molar concentration

Figure 3 shows the gas composition and yield as a function of molar concentration. The main components of the gases were H_2, CO, CO_2 and CH_4. Obviously, the H_2 yield increased and greenhouse gases (CO, CO_2 and CH_4) decreased as the molar concentration of sodium hydroxide increase. At 1.0 M of sodium hydroxide, the result showed the highest hydrogen yield and the lowest greenhouse gases. It is believed that OH and H free radical species attacked and decomposed cellulose molecules easily at the highest molar concentration of sodium hydroxide. Alkali has a capability to disrupt the structure of cellulose and breaks the linkage [6].

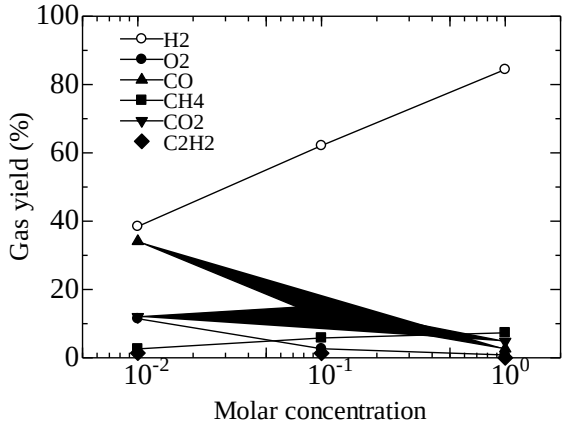

Figure 3 The produced gas compositions as a function of molar concentration of sodium hydroxide.

Figure 4 shows the effect of molar concentration of sodium hydroxide on the hydrogen production rate. It can be described that at specific residence time, an increase in molar concentration resulted in an increase of hydrogen production rate. On the other hand, it is noted that regardless of molar concentration, the hydrogen production rate significantly dropped with residence time. The decreased was expected due to the less efficient for producing radical species by plasma.

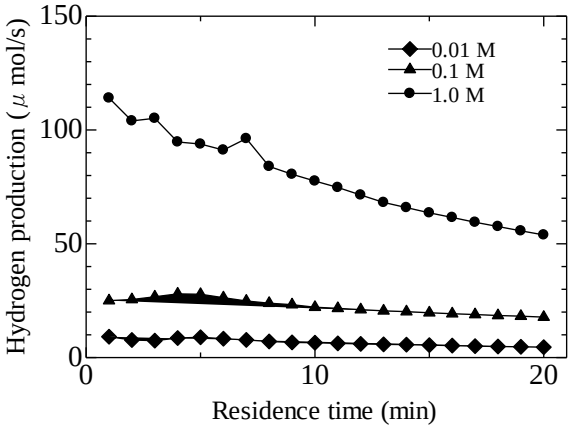

Figure 4 The change of hydrogen production rate with the difference of sodium hydroxide molar concentration.

4. CONCLUSION

In this study the effects of alkali with residence time of plasma discharge was carried out. Plasma in liquid generated Hα (656.3 nm), H_β (486 nm), OH (281.1 nm) and O (777 and 845 nm) free radical species. The dominant spectrums were Hα and OH. The plasma electron temperature was approximately 4200 K. The higher the residence time, the lower the intensity of radical species. At 1.0 M of sodium hydroxide, the result showed the highest hydrogen yield and the lowest greenhouse gases. Besides, at specific residence time, an increase in molar concentration resulted in an increase of hydrogen production rate. On the other hand, it is noted that regardless of molar concentration, the hydrogen production rate significantly dropped with residence time.

REFERENCES

[1] Nomura, S., & Toyota, H. (2003). Sonoplasma generated by a combination of ultrasonic waves and microwave irradiation. *Applied Physics Letters*, *83*(22), 4503-4505.

[2] Mukasa, S., Nomura, S., Toyota, H., Maehara, T., Abe, F., & Kawashima, A. (2009). Temperature distributions of radio-frequency plasma in water by spectroscopic analysis. *Journal of Applied Physics*, *106*(11), 1-6.

[3] Syahrial, F., Nomura, S., Mukasa, S., Toyota, H., & Okamoto, K. (2015). Synergetic effects of radio-frequency (RF) in-liquid plasma and ultrasonic vibration on hydrogen production from glucose. *International Journal of Hydrogen Energy*, *40*(35), 11399-11405.

[4] Maehara, T., Toyota, H., Kuramoto, M., Iwamae, A., Tadokoro, A., Mukasa, S., Yamashita, H., Kawashima, A., & Nomura, S. (2006). Radio frequency plasma in water. *Japanese journal of applied physics*, *45*(11R), 8864.

[5] Rehman, F., Lozano-Parada, J. H., & Zimmerman, W. B. (2012). A kinetic model for H2 production by plasmolysis of water vapours at atmospheric pressure in a dielectric barrier discharge microchannel reactor. *international Journal of Hydrogen Energy*, *37*(23), 17678-17690.

[6] Syahrial, F., Tange, K., Nomura, S., Mukasa, S., & Toyota, H. (2017). Investigation on the effects of ultrasonic irradiation and sodium hydroxide on decomposition of cellulose using rf plasma in liquid for hydrogen production at atmospheric pressure. *Journal of the Japan Institute of Energy, 96*(10), 451-455.

Designing a solar collector using f-chart method for domestic hot water in Malaysia

Fatiha Abdul Rahman[1], Mohd Afzanizam Mohd Rosli[1,2,*], Danial Shafiq Mohd Zaki[1]

[1)] Faculty of Mechanical Engineering, Universiti Teknikal Malaysia Melaka, Hang Tuah Jaya, 76100 Durian Tunggal, Melaka, Malaysia.
[2)] Centre for Advanced Research on Energy, Universiti Teknikal Malaysia Melaka, Hang Tuah Jaya, 76100 Durian Tunggal, Melaka, Malaysia.

[*]Corresponding e-mail: afzanizam@utem.edu.my

Keywords: F-chart method; solar collector; water heating system

ABSTRACT – The solar energy system converts solar energy into useful energy. The performance system depends on the weather that changes over period of time. In this study, the f-chart method was used to predict the solar collector system. The f-chart method is one of the empirical frameworks that use metric standards to characterize the long-term performance of the solar system. A total of 3 varied sizes of solar collectors were used in this study. Residential areas in Bangi have been selected to design hot water heating systems using solar energy using the environment data in 2013. After doing this study, the load given by the solar collector for 3 varied sizes is not the same as 0.38, 0.66 and 0.84. This shows that 0.84 is the highest and shows that 84% of the load is supplied by solar energy. The monthly average domestic heating in Malaysia is 1.22 GJ. Meanwhile, the total domestic heating temperature in Malaysia is 14.66 GJ.

1. INTRODUCTION

The method called f-charts is one of the empirical frameworks that uses standardised metrics to characterise the long-term performance of solar system. Nowadays many researchers are using F-chart method because of its simple analytical formulation, as opposed to an annual full- time transient simulation performed in codes such as TRNSYS [1]. Other than that, f-chart method is the simplest method to determine the size of the solar collector [2]. The parameters range for the f-chart method is applicable are limited because the f-chart method was developed only for standard type of solar space and domestic water heating systems [3].

2. METHODOLOGY

For this project, three different solar collectors were selected to be analyze. The selection based on the availability in the Malaysia market. Table 1 shows the characteristics of all the collectors that used in this project. The $F_R U_L$ for all collectors are the same which is 4.00 (W/m²). It refer to the collector coefficient heat losses to the surrounding from top, bottom and edges of collector. The collector heat exchanger correction factor also are the same for all three of the collectors, there are three different collector areas, the $F_R(\tau\alpha)_n$ same for all the collectors. It refer the transmittance and absorption of collector of irradiance. The $\frac{(\overline{\tau\alpha})}{(\tau\alpha)_n}$ a bit different for all collectors.

Table 1 Characteristics of the collector.

Characteristics	Collector 1	Collector 2	Collector 3
$F_R U_L$ (W/m²)	4.00	4.00	4.00
$\frac{F'_R}{F_R}$	0.97	0.97	0.97
A_c (m²)	2	4	6
$F_R(\tau\alpha)_n$	0.74	0.74	0.74
$\frac{(\overline{\tau\alpha})}{(\tau\alpha)_n}$	0.94	0.96	0.94

2.1 Calculation

This case study uses all the equation below:

1. Monthly water heating load. Where $L_w$is monthly total heating load for space heating and hot water, C_p is specific heat of water, ρ is density of water, h_w is hot water daily consumption, T_w is required hot water temperature which is 80°C, T_m is Mains water supply temperature and N is number of days in the month

$$L_w = C_p \rho h_w (T_w - T_m) N \quad (1)$$

2. Value of x and y

i) For x

$$= F_R U_L \times \frac{F'_R}{F_R} \times (T_{ref} - \overline{T}a) \times \Delta t \times \frac{A_c}{L} \quad (2)$$

ii) For y

$$= F_R(\tau\alpha)_n \times \frac{F'_R}{F_R} \times \frac{(\overline{\tau\alpha})}{(\tau\alpha)_n} \times \overline{H}_T N \times \frac{A_c}{L} \quad (3)$$

3. Monthly total load supplied by the solar space (f-chart)

$$f = 1.029y - 0.065x - 0.245y^2 + 0.0018x^2 + 0.0215y^3 \quad (4)$$

4. Annual fraction of the load supplied by solar energy

$$F = \frac{\Sigma fL}{\Sigma L} \quad (5)$$

5. Storage capacity for selected solar collector

$$\frac{X_c}{X} = \left(\frac{actual\ storage\ capacity}{standard\ storage\ capacity}\right)^{-0.25} \quad (6)$$

3. RESULTS

The monthly water heating load, Value of x, y and *f*, annual fraction of the load supplied by solar energy, and Storage capacity for selected solar collector are shown in Table 2 to Table 5 and Figure 1.

Table 2: Monthly heating load, L.

Month	Heating load, L (GJ)
January	1.25
February	1.14
March	1.24
April	1.19
May	1.22
June	1.18
July	1.25
August	1.25
September	1.21
October	1.25
November	1.22
December	1.26

Table 3 Value of x and y for collector 3.

Month	X	Y	*f*
January	3.65	1.31	0.76
February	3.64	1.58	0.89
March	3.65	1.49	0.85
April	3.67	1.64	0.91
May	3.67	1.67	0.92
June	3.68	1.66	0.92
July	3.66	1.75	0.95
August	3.64	1.46	0.83
September	3.65	1.43	0.82
October	3.65	1.41	0.81
November	3.64	1.21	0.71
December	3.64	1.25	0.73

*Value of *f* by using chart (January)

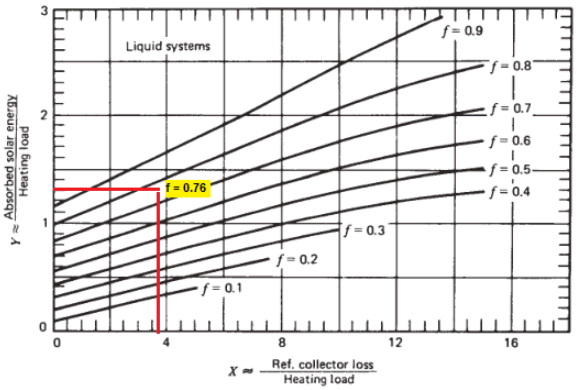

Figure 1 The f-Chart for systems using liquid heat transfer and storage media collector 3.

Table 4 The annual fraction of the load supplied for collector 3.

Month	L, GJ	*f*	*f*L, GJ
January	1.25	0.76	0.95
February	1.14	0.89	1.01
March	1.24	0.85	1.05
April	1.19	0.91	1.08
May	1.22	0.92	1.12
June	1.18	0.92	1.09
July	1.25	0.95	1.19
August	1.25	0.83	1.04
September	1.21	0.82	0.99
October	1.25	0.81	1.01
November	1.22	0.71	0.87
December	1.26	0.73	0.92
Total	14.66		12.32

$$F = \frac{12.32}{14.66} = 0.84 \times 100 = 84\%$$

This indicates that 84% of the annual load is supplied by solar energy.

Table 5 The annual fraction of the load supplied by a storage size correction for collector 3

Month	L, GJ	*f*	*f*L, GJ
January	1.25	0.80	1.00
February	1.14	0.93	1.06
March	1.24	0.89	1.10
April	1.19	0.95	1.13
May	1.22	0.96	1.17
June	1.18	0.96	1.13
July	1.25	0.99	1.24
August	1.25	0.87	1.09
September	1.21	0.86	1.04
October	1.25	0.85	1.06
November	1.22	0.75	0.92
December	1.26	0.77	0.97
Total	14.66		12.91

F=12.91/14.66 0.88×100=88%

The annual load supplied by solar energy after size correction is 88%. This because Malaysia is located in the equatorial region, being hot and humid throughout the year. Besides, Malaysia also exposed to the El Nino effect, which reduces the rainfall in dry season. Peninsular Malaysia known as hottest state in Malaysia with the average 12 hours of sunlight received per day. This can have affected the solar collector to receive the solar radiation along with the large surface area of the solar collector.

4. CONCLUSION

As a conclusion, found that the annual load that supplied by solar energy for the selected solar collector which is 84%. The average monthly heating load of domestic hot water in Malaysia which is 1.22 GJ. Meanwhile, for the total annual heating load of domestic hot water in Malaysia is 14.66 GJ. The annual fraction of the load supplied by a storage size correction is 88%.

REFERENCES

[1] Koussa, M., & Djohra, S. (2014, March). Long term PV system performances estimating by using only the main weather parameters data. Case of study: An Algerian Temperate climate. *Renewable Energy Congress (IREC),* 1-6.

[2] Duffie, J.A. and Beckman, W.A., *Solar Engineering of Thermal Processes Solar Engineering*, 4th ed. Canada: Wiley; 2013.

[3] Okafor, I. F., & Akubue, G. (2012). F-chart method for designing solar thermal water heating systems. *International Journal of Scientific & Engineering Research*, *3*(9), 1-7.

Preliminary study of computational fluid dynamics on photovoltaic thermal solar air collector

Yap Joon Ping[1], Mohd Afzanizam Mohd Rosli[1,2,*], Muhammad Asraf Saruni[1]

[1)] Faculty of Mechanical Engineering, Universiti Teknikal Malaysia Melaka, Hang Tuah Jaya, 76100 Durian Tunggal, Melaka, Malaysia.
[2)] Centre for Advanced Research on Energy, Universiti Teknikal Malaysia Melaka, Hang Tuah Jaya, 76100 Durian Tunggal, Melaka, Malaysia.

[*]Corresponding e-mail: afzanizam@utem.edu.my

Keywords: Photovoltaic thermal collector; CFD

ABSTRACT – The purpose of this research is to investigate the efficiency of PV/T located in India and Malaysia. ANSYS Fluent software was used to carry out computational fluid dynamics (CFD) simulation. In this preliminary study, air was selected as the heat transfer fluid. The geometric model was drawn in CATIA V5R16 and imported into ANSYS software to generate mesh model. In setup, the sun direction, direct normal irradiation and diffuse solar irradiation are inputs generated from the solar calculator by referring to the coordinates of Malaysia and India. The outlet air and PV temperatures obtained can be used to calculate total efficiency. The higher the mass flow rate, the higher the total efficiency.

1. INTRODUCTION

Photovoltaic Thermal (PV/T) system is the combination of photovoltaic system and solar thermal system. PV/T system is capable of converting solar radiation into electrical energy and thermal energy simultaneously.

Conventional photovoltaic (PV) panel only utilizes photon from light to generate electrical energy, however the heat from solar radiation tends to increase the PV panel temperature and reduce its electrical efficiency [3]. Photons of longer wavelength do not generate electron-hole pairs but only dissipate their energy as heat in the PV cell. PV/T system able to extract the heat from PV panel by using heat transfer fluid such as water and air. This cools down the PV panel to provide a better efficiency. The heat gain by heat transfer fluid can be used for space heating and water heating.

Senthil Kumar et al. [1] have conducted a simulation to compare the simulation and experimental results. The research proved that the results which was obtained from the computational fluid dynamics (CFD) method is almost identical to experimental results.

The objective of this research is to investigate the outlet temperature of heat transfer fluid and photovoltaic cell temperature with different mass flow rate in India and Malaysia. Heat transfer fluid used in this research is air. The simulation was performed in steady state condition. Glazed photovoltaic thermal collector model is selected for CFD simulation.

2. RESEARCH METHODOLOGY

2.1 Geometry modelling

In this research, CATIA was employed to draw the PV/T model. The top-down arrangement of the PV/T is top glass, EVA, PV cell panel, tedlar and followed by air duct. Figure 1 shows the arrangement of PV/T air. The dimensions of the layers of air PV/T is shown in Table 1.

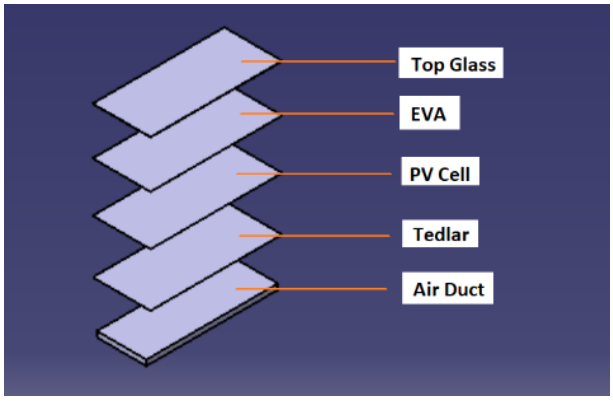

Figure 1 Arrangement of PV/T air.

Table 1 Dimensions of PV/T parts.

Parts of PV/T	Dimensions (m)
Top Glass	1.2 x 0.527 x 0.003
EVA	1.2 x 0.527 x 0.0005
PV Cell Panel	1.2 x 0.527 x 0.0003
Tedlar	1.2 x 0.527 x 0.0005
Air Duct	1.2 x 0.45 x 0.05

2.2 Meshing

Meshing can be defined as a process to divide the geometry into discrete cells. In this research, automatic meshing was used. The relevance centre was set to 'fine' and smoothing was set to 'high'. The mesh model consists of 74868 nodes and 11592 elements. The elements of mesh were in hexahedral shapes as shown in Figure 2.

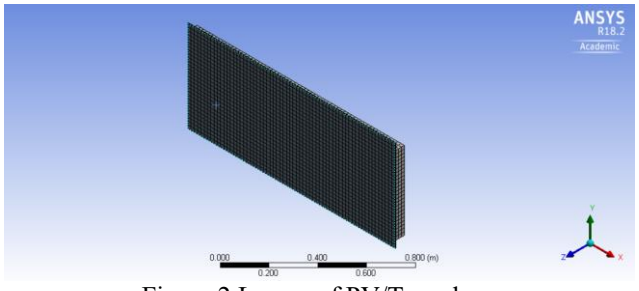

Figure 2 Layers of PV/T mesh.

2.3 Setup and solution

The PV/T and its surrounding conditions were constructed. The k- epsilon model was chosen as the turbulent model for this simulation. The energy equation is applied to allow the calculation of heat transfer. Surface to surface (S2S) was selected for radiation model. The direction and intensity of solar radiation were determined by inserting the coordinates and date into the solar calculator. Table 2 shows the material for every layer of PV/T used in CFD simulation. In validation and verification, the velocity of inlet was set to 10m/s.

Table 2 Material properties of layers of PV/T.

Layers of PV/T	Density (kg/ m^3)	Specific heat capacity (J/kg.K)	Thermal conductivity (W/m.K)
Top glass	2450	500	2
EVA	950	2090	0.311
PV cell	2330	677	130
Tedlar	1200	1250	0.15

3. VALIDATION AND VERIFICATION

Validation and verification were conducted by referring to the previous research [1]. The coordinates of location used in simulation was India.

From Figure 3, it shows the experimental and simulation results from 8a.m. to 5p.m. on a specific day of April. The difference of the outlet temperature between current and previous research simulation results varied from 0.43% to 9.33%. The highest percentage difference was 9.33% which was lower than 10%, therefore this method was validated.

The difference of the outlet temperature between current research simulation results and previous research experimental results varied from 0.22% to 6.89%. The highest percentage error was 6.89%. Hence, this method was verified.

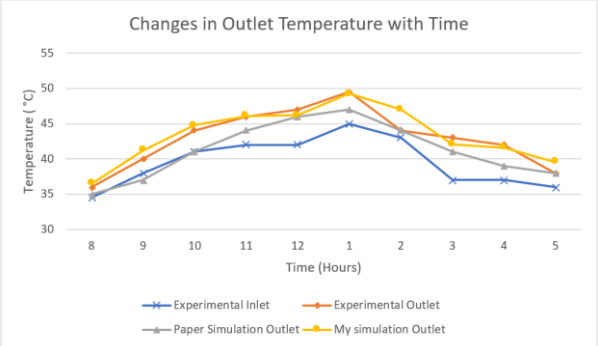

Figure 3 Changes in outlet temperature with time.

4. RESULTS AND DISCUSSION

A simulation was carried out to obtain the outlet air temperature and PV temperature with varying mass flow rate in India and Malaysia. Figure 4 represents the outlet temperature and PV temperature in India and Malaysia while Figure 5 illustrates the change in thermal, electrical and total efficiencies with varying mass flow rate.

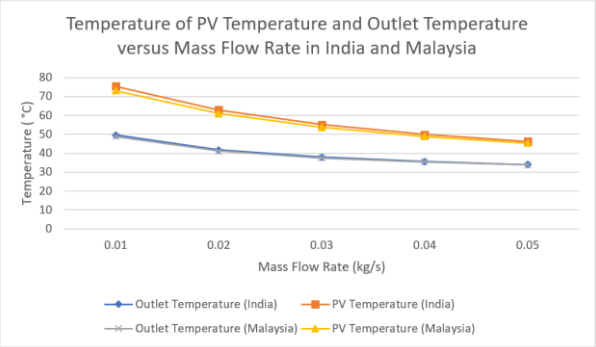

Figure 4 Changes in outlet and PV temperature with mass flow rate in india and Malaysia.

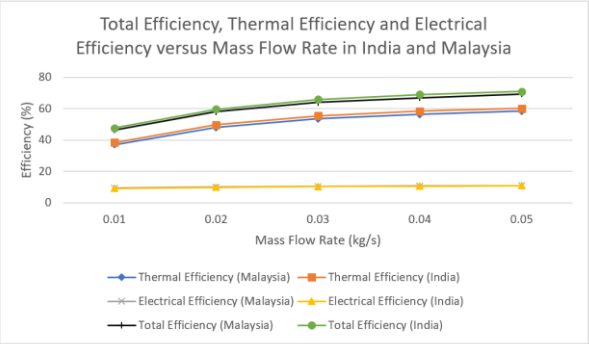

Figure 5 Changes in total efficiency, thermal efficiency and electrical efficiency with mass flow rate in India and Malaysia.

The PV/T was simulated in Madhya Pradesh, India with the coordinates of 20.5937° N, 78.9629° E and Kuala Lumpur, Malaysia with coordinates 3.1390° N, 101.6869° E. The direction and intensity of solar radiation varied by the coordinates and date by using the solar calculator in ANSYS Fluent. The date and time inserted into the solar calculator is 21st April, 1p.m.

The results clearly show that as the mass flow rate was increasing, the PV temperature and outlet air temperature were decreasing. The highest total efficiencies for Malaysia and India obtained were at 0.05kg/s which were 69.32% and 70.95% respectively. The results of PV/T located at India and Malaysia did not have any significant differences. The highest percentage difference for both locations in total efficiency was 3.08% only which is at 0.04kg/s.

5. CONCLUSION

The CFD Fluent method is applicable for the simulation of PV/T air. With the 10 m/s inlet velocity of air, the percentage difference between simulation results of this research and simulation results of previous research and percentage error between simulation results of this research and experimental results of previous research were less than 10%.Based on the results obtained, the higher the mass flow rate, the larger amount of heat is transferred from PV to air, therefore the higher the total efficiency.

ACKNOWLEDGEMENT

This project is supported by Faculty of Mechnical Enginerring, Universiti Teknikal Malaysia Melaka.

REFERENCES

[1] Senthil Kumar, R., Puja Priyadharshini, N., & Natarajan, E. (2015). Experimental and computational fluid dynamics (CFD) study of glazed three dimensional PV/T Solar panel with air cooling. *Applied Mechanics and Materials*, *787*, 102–106.

[2] Chow, T. T. (2010). A review on photovoltaic/thermal hybrid solar technology. *Applied Energy*, *87*(2), 365–379.

[3] Khelifa, A., Touafek, K., Moussa, H., Tabet, I., hocine, H. and Haloui, H. (2015). Analysis of a Hybrid Solar Collector Photovoltaic Thermal (PVT). *Energy Procedia*, 74, pp.835-843.

Preliminary determination of pipe fouling effect for office building cooling tower energy performance

Imanurezeki Mohamad[1,*], Ahmad Anas Yusof[2], Nurul Adzura Ismail[2], Al-Khairi Mohd Daud[3], Hayati Abdullah[4], Md Razali Ayob[2]

[1)] Office of Asset and Development, Universiti Teknologi Malaysia, 81310 Skudai, Johor, Malaysia.
[2)] Faculty of Mechanical Engineering, Universiti Teknikal Malaysia Melaka, Hang Tuah Jaya, 76100 Durian Tunggal, Melaka, Malaysia.
[3)] Faqeh Management, Suite 1208, Level 12, Amcorp Tower, Amcorp Trade Centre, No. 18, Persiaran Barat, 46050, Petaling Jaya, Malaysia.
[4)] Center for Teaching and Learning, Universiti Teknologi Malaysia, 81310 Skudai, Johor, Malaysia.

[*]Corresponding e-mail: imanurezeki@utm.my

Keywords: Building management; energy consumption; cooling tower

ABSTRACT – This study aimed to conduct an experimental analysis to investigate the effect of fouling on the cooling tower piping system. The comparison is made between Galvanised (GI) pipe and Polyvinyl chloride (PVC) pipe. Results found that water resistance for PVC pipe is approximately 5 % lower than GV pipe. The present results show that the pipe materials and diameters will influent the flow rate that also has the detrimental effect on fouling rate and fouling factor. The result from this preliminary study can be used as one of the indicator to evaluate cooling tower system efficiency for the office building.

1. INTRODUCTION

General office building cooling towers (CT) operation is based on evaporation cooling that involves the heat transfer process through a condenser system. The heat transfer process is based on the recirculating of the exhaust heat and is accomplished by maximizing the piping surface area of the water as it flows over and down through the tower structure. However, the main barrier to the CT piping system has increased attention and has been recently researched on the fouling and it effects to the CT performance [1, 2, and 3]. Within this context, fouling in the CT piping system refers to the formation of scale deposit layer on piping system that will cause the accumulation of corrosion. The degree to which fouling will affects the CT piping systems also related to the piping dimensions, piping material, chemical treatments and decomposition of sludge, rust and/or corrosion [2].

In some circumstances, fouling will inhibit the cooling process and affect the cooling tower sub-system operation such as condenser and compressor by restricted the heat exchangers process and thermal resistance by decreasing the water and air flow rate through the tower and will lower the cooling range, respectively [1,3]. Although, water quality issues also have such significant influence of fouling it is beyond the scopes of this study.

Therefore, this study focuses on fouling effect of the cooling tower piping system. In this study, fouling effects are evaluated from the efficiency of water flow rate and friction factor. This study also compared the fouling effects of GI pipe and PVC pipe. The results of this study will be used as the preliminary indicator to further evaluate CT system efficiency and identify future energy saving potential for the selected office building.

2. METHODOLOGY

The central cooling tower database of the Bangunan Canseleri Sultan Ibrahim (BCSI) management building of Universiti Teknologi Malaysia main Campus is used to support the development and implementation of this study. The present experimental work is conducted with a varied water mass flow rate between 100 to 550 gal/minutes through 3 to 5 inches of pipe dimensions and constant water and the air temperature of 38ºC and 30ºC, respectively.

The flow rate performance of both pipes was recorded and compared. The data points are collected for a 1 min sampling rate. Total water use for the cooling tower can be calculated as Equation (1) [2].

$$M_u = E + B_D + D + L \quad (1)$$

Where, M_u is the make-up water of the cooling tower, E is the evaporation rate, B_D is the system blowdown rate, D is the estimated drift and wind loss rate that can account for less than 0.001% of water use and L is the rate of leaks, overflows, and other losses that should be controllable with proper fill valves and routine maintenance [3].

The basic relationship of fouling deposition on surfaces from a moving fluid is defined based on Equation (2). The rate of deposit growth known as fouling resistance or fouling factor, R_f.

$$R_f = \Phi_d - \Phi_r \quad (2)$$

Where, Φ_d and Φ_r are the rates of deposition and removal, respectively. The fouling factors, R_f is expressed in terms of thermal resistance as m^2. k/w or in the units of the thickness change as m/s or units of mass change as $kg/m^2.s$.

The frictional pressure drop in the tube for a single phase flow can be determined from Equation (3).

$$\Delta P = 4f\left(\frac{L}{d_i}\right)\frac{\rho\mu_m^2}{2} \quad (3)$$

Where f is the fanning friction factor, L indicates the

tube's length, $d_i$is the inner diameter and μ_m is the fluid velocity.

The fanning friction factor for a fluid in a laminar flow, circulating within circular tubes, independent of the surface roughness, can be simply defined as stated in Equation (4).

$$f = \frac{16}{R_e} \quad (4)$$

Therefore, the effect of flow rate on the surface fouling is defined in Equation (5).

$$R_f = A.\frac{1}{u}\left(1 - e^{-\theta/\theta_c}\right) \quad (5)$$

Where u is a surface parameter, θ_c is a time constant and A is the lumped parameters defined from experimental data. Then, the fouling built up rate quantified as deposit thickness increase per unit time as shown in Equation (6).

$$Foulant\ BuildUp\ Rate = \frac{T_2 - T_1}{t_2 - t_1} \quad (6)$$

Where, T_1 and T_2 is deposit thickness measured at the previous and current inspections, respectively. The time elapsed between is quantified by $T_2 - T_1$.

3. RESULTS AND DISCUSSION

The experimental results, as shown in Figures 1 to 3 depicted that the variable flow rate higher with increasing pipe dimensions. The results shown in Figures 1 to 3 illustrated that the friction loss is also less affected by using PVC pipe than a GI pipe, this is partly due to the fact the constant water flow rate suffer loses due to friction. The water resistance for PVC pipe is approximately 5 percent lower than GV pipe will influent the flow rate that also has the detrimental effect on fouling rate and fouling factor. As suggested by Qurashi and Zubair [3] the capital investment for equipment for could be greatly reduced for power utilities which could be reflected in less expensive energy consumption. In this case, they stated that evaluation of the cooling system can be used as an optimization tool for best overall cooling system efficiency at various load and ambient conditions.

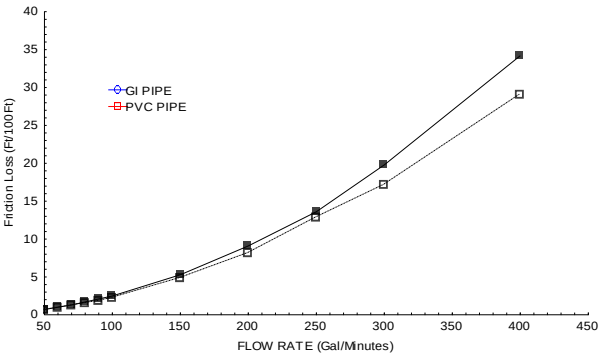

Figure 1 Friction loss for 3 in. pipe diameter.

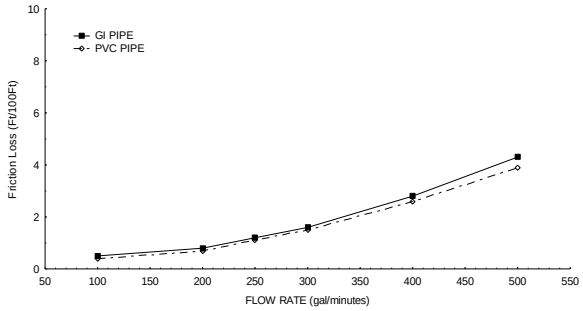

Figure 2 Friction loss for 4 in. pipe diameter.

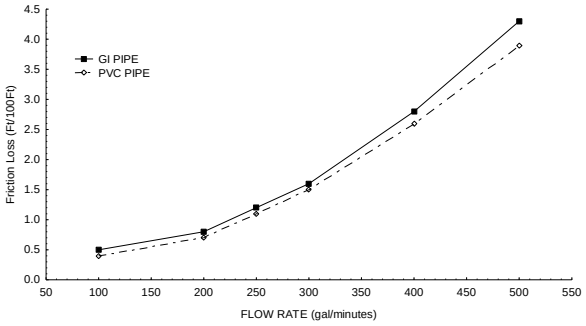

Figure 3 Friction loss for 5in. pipe diameter.

4. CONCLUSION

This study found that PVC pipe performs better in term of flow rate and friction loss than GI pipe. Based on this experimental study, the difference in inside cross-sectional area, wet surface, and roughness of the surface that contribute to the difference in friction head loss in GI and PVC pipes will influent the flow rate that also has the detrimental effect with fouling rate and fouling factor. Consequently, this study had a relatively small sample size and the building sample is not completely representative, these findings should be confirmed by a larger study.

ACKNOWLEDGEMENT

This study is carried out at Universiti Teknologi Malaysia under the financial support of Yayasan Sarawak).

REFERENCES

[1] Awad, M. M. (2012). Impact of flow velocity on surface particulate fouling–theoretical approach. *Journal of American Science*, *8*(9), 442-449.

[2] Sullivan, G., Pugh, R., Melendez, A. P., & Hunt, W. D. (2010). *Operations & Maintenance Best Practices-A Guide to Achieving Operational Efficiency (Release 3)* (No. PNNL-19634). Pacific Northwest National Laboratory (PNNL), Richland, WA (US).

[3] Qureshi, B. A., & Zubair, S. M. (2006). A complete model of wet cooling towers with fouling in fills. *Applied Thermal Engineering*, *26*(16), 1982-1989.